Protein Nanofibrils

DOI: 10.1002/ange.201006859

Photoelectric Protein Nanofibrils of α-Synuclein with Embedded Iron and Phthalocyanine Tetrasulfonate**

*Yeon Sun Choi, Jehoon Kim, Ghibom Bhak, Daekyun Lee, and Seung R. Paik**

The development of photoelectric systems that respond to visible light has gained a great deal of attention for the preparation of light-harvesting and optical-switching systems, which would contribute to the construction of sensors, electronics, optical information processing systems, and energy-transducing devices.[1–3] Porphyrinic molecules are considered to be ideal for the photoinduced electron-transfer process owing to their excellent photonic, electronic, and catalytic properties.[4–6] To harness these properties in a more effective and practical way, their hierarchical suprastructures have been engineered to give rise to controlled spatial arrangement of the unique aromatic compounds by taking advantage of their self-interactive property.[7–9] Herein, we demonstrate selective localization of the porphyrinic compound phthalocyanine tetrasulfonate (PcTS) into a protein matrix of amyloid fibrils made of α-synuclein in the presence of iron, which results in conversion of the dielectric protein nanofibrils into light-inducible conductive hybrid nanomaterials.

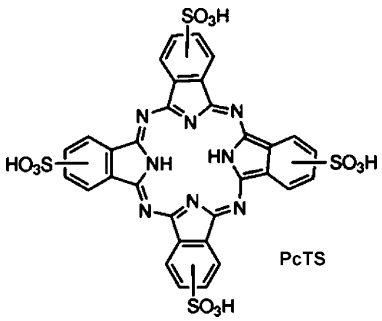

PcTS

Although multifunctional hybrid molecules can be generated by decorating biomolecules such as proteins and nucleic acids,[10–14] their functions are fully exploited when they are organized into well-defined suprastructures such as one-dimensional fibrils, two-dimensional sheets/films, or three-dimensional matrices. By providing nanofibrillar templates, amyloid fibrils can be considered as one of the best candidates to prepare the functional suprastructures. Amyloid fibrils, mostly known as a common pathological component of various neurodegenerative disorders including Parkinson's and Alzheimer's diseases, are protein nanofibrils with an average width of 10–20 nm.[15,16] The amyloid fibrils derived from a molecular self-assembly process of soluble amyloidogenic proteins exhibit a mechanical strength comparable to that of spider silk by forming a cross β-sheet conformation.[15] In addition, application of the nanofibrils has also been suggested in the areas of nanobiomedicine and nanoelectronics by providing basic materials for biosensors, microfluidics, drug delivery, and conductive nanowires.[15,17–21]

The multipotential compound PcTS has been integrated into amyloid fibrils of α-synuclein in the presence of iron by employing a typical bottom-up fabrication strategy for nanoarchitecture formation. α-Synuclein is the major constituent of Lewy bodies, a pathological hallmark of Parkinson's disease, as it forms radiating filamentous structures of amyloid fibrils.[22–24] Recently, we have demonstrated that the protein was fibrillated by a unit-assembly process of its oligomeric granular species in the presence of shear force or the organic solvent hexane.[25,26] To create the photoelectric hybrid nanoscale fibrils, the unit-assembly phenomenon was thus employed by preparing an oligomeric species of α-synuclein with Fe^{3+} and subsequently connecting the metal–protein units with PcTS (Scheme 1). In fact, this proposed strategy was previously tested by producing PcTS-mediated nanofibrils of Aβ1-40, another pathological amyloidogenic peptide found in the senile plaques of Alzheimer's disease, which resulted in concomitant reduction in the cytotoxicity of the iron-induced oligomeric Aβ1-40.[27]

The building block of the oligomeric species of α-synuclein was prepared with $FeCl_3$ (0.2 mM). α-Synuclein (α-Syn, 0.288 mg mL^{-1}) was incubated in 4-morpholineethanesulfonic acid hydrate (Mes; 20 mM, pH 6.5) in the presence or absence of Fe^{3+} at 37 °C with shaking by an orbit shaker running at 200 rpm. Under these conditions, the fibrillation of α-synuclein was consistently suppressed by the metal ion with a lag period extended twofold, as well as a reduced final thioflavin-T binding fluorescence to half of the fibrillation kinetics obtained in the absence of iron (Figure 1a). When the final fibrils were examined by transmission electron microscopy (TEM) after negative staining with uranyl acetate (2%), normal amyloid fibrils of α-synuclein obtained without Fe^{3+} (Figure 1b) became shortened to an average length of (90 ± 24) nm (Figure 1c) as the metal ion was included in the fibrillation process.

[*] Y. S. Choi, J. Kim, G. Bhak, Dr. D. Lee, Prof. S. R. Paik
School of Chemical and Biological Engineering
College of Engineering, Seoul National University
Seoul 151-744 (Korea)
E-mail: srpaik@snu.ac.kr
Homepage: http://apml.snu.ac.kr/

[**] This research was supported by the Basic Science Research Program through the National Research Foundation of Korea (NRF) funded by the Ministry of Education, Science, and Technology (2010-0009809).

Supporting information for this article (details of materials and experimental procedures) is available on the WWW under http://dx.doi.org/10.1002/anie.201006859.

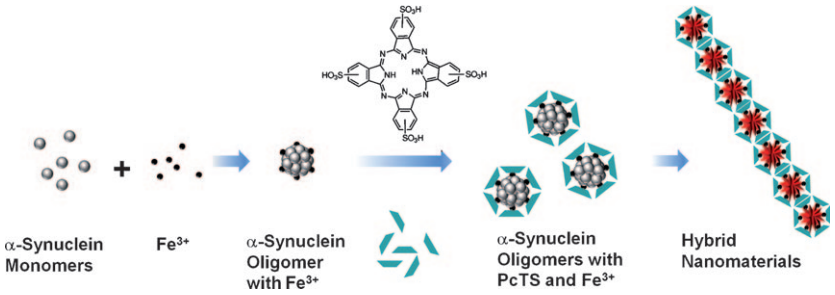

Scheme 1. Photoelectric hybrid protein nanofibril preparation by using the iron/PcTS-mediated unit-assembly process of α-synuclein.

straight fibrils with a maximum length of 1.4 μm; these fibrils also exhibited the unique characteristic of tightly packed 2D fibrillar alignment (Figure 2a, middle). In the absence of iron, however, PcTS alone caused the α-synuclein oligomers to assemble into randomly oriented curly fibrillar structures (see the Supporting Information, Figure S1). These data, therefore, clearly demonstrate that the PcTS-induced hybrid nanofibrils exhibit a fibrillar polymorphism depending on the oligomeric state of α-synuclein prepared with Fe^{3+}.

The remarkable 2D fibrillar alignment derived from the iron-induced 10-hour oligomers of α-synuclein was demon-

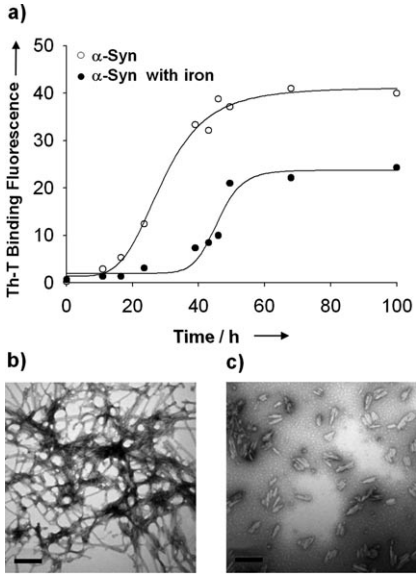

Figure 1. Fibrillation of α-synuclein in the presence and absence of iron. a) Fibrillation kinetics monitored with thioflavin-T (Th-T) binding fluorescence. α-Syn was incubated in the absence or presence of $FeCl_3$. b, c) Morphologies of the α-synuclein fibrils obtained without (b) and with (c) iron. Scale bars: 200 nm.

The oligomeric species of α-synuclein obtained with iron were collected at three different time points of 5, 10, and 20 h during the lag period of the α-synuclein (20 μM) fibrillation with Fe^{3+} (0.2 mM). PcTS (0.2 mM) was added to the oligomers appearing indistinguishable under TEM (Figure 2), to initiate the PcTS-mediated unit-assembly process for a total incubation period of 100 h from the beginning of fibrillation. Intriguingly, the final morphologies of the PcTS-induced nanofibrils were revealed distinctively with respect to their shape, length, and mutual alignment (Figure 2a).

The PcTS-induced protein nanofibrils obtained with the 5-hour oligomers were 400–800 nm long and exhibited occasional bent structures without discernable fibrillar alignment (Figure 2a, top). The fibrils with the 20-hour oligomers did not extend as much, which resulted in rather short fibrils with an average length of (70 ± 27) nm. These straight fibrils often existed in two to three adjoining strands (Figure 2a, bottom). The 10-hour oligomers, on the other hand, formed extraordinary suprastructures with PcTS and revealed fully extended

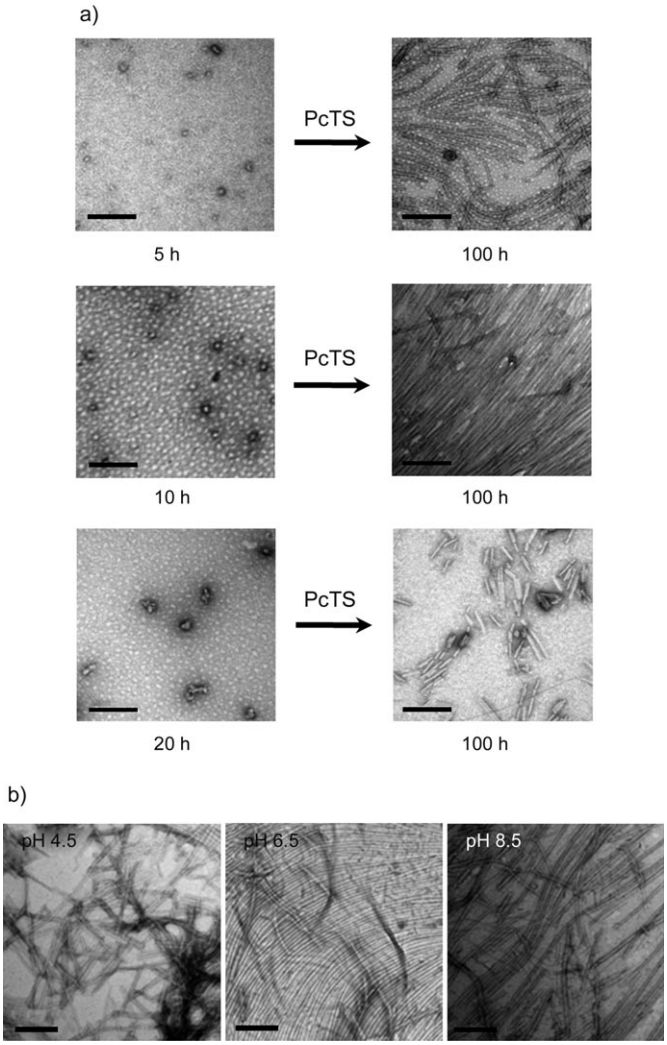

Figure 2. PcTS-induced fibrils from Fe^{3+}-mediated oligomers of α-synuclein and their pH-dependent 2D alignment. a) Oligomers obtained at three different time points from the incubation of α-synuclein and $FeCl_3$ were further incubated for a total of 100 h with PcTS under the same conditions. b) pH effect on the 2D fibrillar alignment of the iron–PcTS-containing α-synuclein fibrils. The fibrils were prepared in a complex buffer made of 20 mM each of citrate, Mes, Tris–HCl, and glycine, and by adjusting the pH value to 4.5, 6.5, or 8.5 with either 1 N HCl or 1 N NaOH. Scale bars: 200 nm.

strated to be pH-dependent. The fibrils formed a 2D array only at pH 6.5, while their tendency for mutual alignment disappeared at either pH 4.5 or 8.5 (Figure 2b). This fact may indicate that the fibrillar alignment is mediated by the adjoining PcTS in addition to α-synuclein.

Specific incorporation of PcTS into the fibrils in the presence of Fe^{3+} was evaluated by both CD and UV/Vis spectroscopy. The CD spectra showed that the α-synuclein monomer existed in a random structure with minimum ellipticity at 200 nm. The α-synuclein fibrils prepared in the presence or absence of iron and PcTS revealed a β-sheet conformation, although the wavelength of minimum ellipticity changed from 221 to 216 nm as the PcTS and iron were incorporated into the fibrils (Figure 3a). This might imply

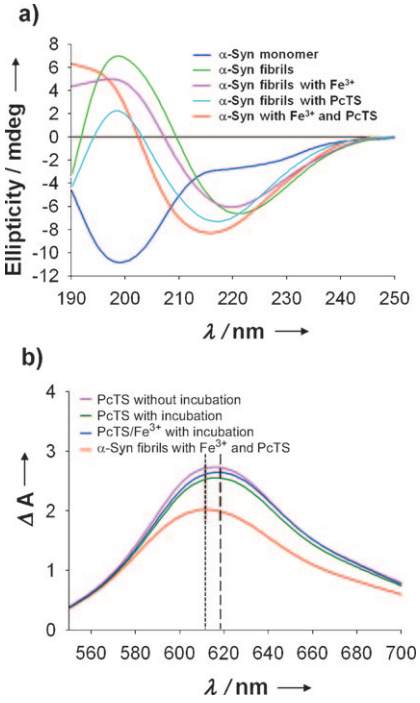

Figure 3. CD and UV/Vis spectra of the Fe^{3+}–PcTS-containing fibrils of α-synuclein. a) CD spectra were obtained for normal amyloid fibrils of α-synuclein and fibrils prepared with Fe^{3+}, PcTS, or Fe^{3+}/PcTS. The spectrum of monomeric α-synuclein is shown as a control. b) UV/Vis spectra of PcTS in the absence or presence of Fe^{3+} or Fe^{3+}/PcTS.

that the Fe^{3+}–PcTS-containing fibrils were also produced through the α-synuclein self-assembly process, although the protein assembly appeared to be modified by the iron and PcTS.

The UV/Vis absorption spectra of the hybrid nanofibrils provided topological information on the intercalated PcTS within the fibrils upon examination of the Q-bands between 500 and 650 nm. The relative orientation of the transition dipole moments determines which energy level absorbs light for the phthalocyanine molecules. As PcTS molecules align through either cofacial or edge-to-edge interaction, they would absorb the radiation to either higher (blueshift) or lower level (redshift) from a fixed electronic level of isolated PcTS, respectively.[28] All the unbound PcTS molecules collected with or without the extended period of incubation of 100 h in the presence or absence of Fe^{3+} gave rise to absorption spectra culminating at 617 nm, while the hybrid nanofibrils of α-synuclein containing Fe^{3+} and PcTS showed a blue-shifted spectrum with a maximum absorbance peak at 611 nm (Figure 3b). The results indicate that PcTS alone did not self-organize into any sort of hierarchical structure under our reaction conditions regardless of the iron. In the presence of α-synuclein, however, the PcTS molecules intercalated into amyloid fibrils with cofacial orientation in the presence of Fe^{3+}, as judged by the blue-shifted spectrum of the hybrid material.

The actual presence of Fe^{3+} and PcTS in the nanofibrils was confirmed by elemental analysis with scanning electron microscopy (SEM) by examining the presence of iron and sulfur atoms (see the Supporting Information, Figure S2). Although the molecular details of α-synuclein, PcTS, and iron in the formation of the hybrid nanofibrillar suprastructures cannot be explicitly unraveled, iron and PcTS coordination appears to play a crucial part in fibril formation and subsequent alignment, since the α-synuclein oligomers resulted in curly amyloid fibrils when they were incubated with PcTS alone in the absence of iron (see the Supporting Information, Figure S1) whereas the protein had rather short amyloid fibrils with iron in the absence of PcTS (Figure 1c). The CD spectra also indicate that the structural characteristic of the hybrid fibrils incorporating both Fe^{3+} and PcTS is distinctive from that of the fibrils generated in the presence or absence of either Fe^{3+} or PcTS (Figure 3a).

The resulting Fe^{3+}/PcTS-mediated α-synuclein protein nanofibrils could be applied as multifunctional hybrid nanofibrils exhibiting both light-harvesting and electron-transfer properties. The conductivity of the hybrid protein fibrils was evaluated by constructing Si wafers on which three different types of α-synuclein fibrils (containing iron, PcTS, or Fe^{3+}/PcTS) were layered by drying. After applying silver paste on both ends of the Si wafer (see the Supporting Information, Figure S3), the conductance was monitored by obtaining current–voltage curves. All three fibril types were able to carry the current as electric potential was applied. As the potential gradually increased, the current they carried increased proportionally to a certain point and then suddenly soared up (Figure 4a). This two-phase current–voltage response was more evident for the hybrid nanofibrils of α-synuclein containing both Fe^{3+} and PcTS than for the fibrils with either Fe^{3+} or PcTS.

The Fe^{3+}–PcTS-containing hybrid nanofibrils exhibited a dramatic transition of the slopes, which represented a conductance (σ) from 44 to 270 AV^{-1}. The first- and second-phase conductance of the Fe^{3+}-containing fibrils was 21 and 75 AV^{-1}, respectively, while the PcTS-containing fibrils showed an augmentation of the conductance from 15 to 139 AV^{-1}. The nanofibrils of α-synuclein containing both Fe^{3+} and PcTS were definitely more conductive than the other two fibril types for both phases. In addition, the two conductances of the Fe^{3+}–PcTS-containing nanofibrils were higher than the corresponding sums of the first and second phases of the other fibrils containing only Fe^{3+} or PcTS. These facts indicate that the co-presence of PcTS and Fe^{3+} within the hybrid fibrils

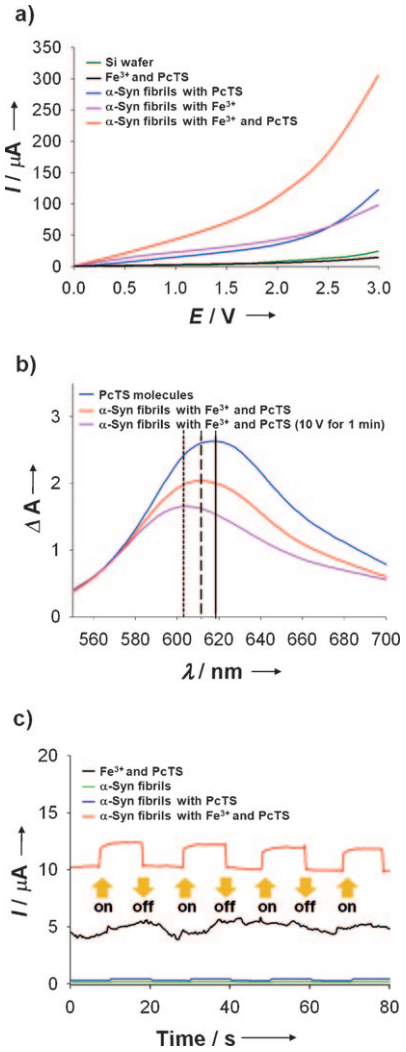

Figure 4. Electrical conductivity and photoelectric response of the Fe^{3+}–PcTS-containing hybrid protein nanofibrils. a) Current–voltage curves of α-synuclein fibrils produced with Fe^{3+}, PcTS, or Fe^{3+}/PcTS. b) UV/Vis absorption spectra of electrically prechallenged Fe^{3+}–PcTS-containing nanofibrils. c) Photoelectric response of the Fe^{3+}–PcTS-containing nanofibrils upon on/off light exposure.

contributes considerably to carrying of the current by possibly providing ion pairs.

A possible explanation for the dramatic increase in conductance of the second phase could be that the conducting substances is reoriented within the fibrillar matrix by the previously applied electric potential. To verify this, the absorption spectrum of the electrically prechallenged hybrid nanofibrils containing both Fe^{3+} and PcTS was monitored. The blue-shifted absorption maximum at 611.5 nm for the Fe^{3+}–PcTS-containing fibrils was further shifted to a shorter wavelength at 604 nm following electrical pretreatment for 1 min at 10 V (Figure 4b). These data suggested that a possible reorientation of the conductive pairs could occur during the less conductive initial phase to exert the enhanced second-phase conductance. In fact, the morphology of the hybrid fibrils at least was shown to be affected from the well-annealed planar surface to the discrete fibrillar meshwork state, as revealed by SEM following electrical pretreatment (see the Supporting Information, Figure S4). Taken together, therefore, the electrically prechallenged hybrid nanofibrils changed their shape by altering the orientation of PcTS molecules and thus the conductivity of the nanofibrils.

The light-harvesting activity of the Fe^{3+}–PcTS-containing conductive hybrid nanofibrils cofacially aligned within the amyloid fibrils was then evaluated, which was reflected in the increased electrical current of the fibrils on a Si wafer upon light exposure with a solar simulator under a constant voltage of 0.5 V. As the light was turned on and off, the hybrid nanofibrils containing both Fe^{3+} and PcTS responded accordingly by increasing the current level by 1.55 mA, which was observed repetitively upon light exposure (Figure 4c). These data clearly demonstrate that the hybrid nanofibrils are capable of harvesting light and subsequently transforming it into electrical signals. In addition, the hybrid nanofibrils were demonstrated to exert a photodynamic effect useful for photodynamic therapy, by monitoring their hydroxyl radical production in the presence of hydrogen peroxide upon laser exposure at 633 nm, which suggests a possible use of the materials to control cellular viability (see the Supporting Information, Figure S5).

Since these hybrid nanofibrils tend to form spontaneous 2D arrays and well-organized materials, which significantly improves their practical value for application by enhancing light absorption, conductivity per area, and material uniformity, the following benefits can be expected in terms of chemical and physical perspectives. The light-harvesting and subsequent electrical-conductivity properties of the hybrid nanofibrils could be improved by additional engineering of the diverse reactive functional groups of the protein through chemical modification. Since the final morphology of the protein suprastructures has been demonstrated to be readily controlled by manipulating the assembly property of α-synuclein,[25,29] it is possible to fabricate various forms of photoelectrical protein hybrid materials. In addition, selective disintegration of the materials could be accomplished by photolysis and possible proteolysis. Therefore, the resulting multifunctional PcTS-containing protein suprastructures could be employed as robust photonic materials for the development of nanodevices requiring photocatalytic, photovoltaic, and photodynamic effects.

In summary, we have successfully prepared well-aligned, conductive, and light-responsive hybrid nanoscale materials by incorporating iron and PcTS into the amyloid fibrils of α-synuclein. The iron-induced oligomeric species of α-synuclein underwent unit assembly mediated by PcTS to form hybrid nanofibrils exhibiting spontaneous 2D array formation, with the photoelectric properties of light harvesting and subsequent transformation into electrical signals. Therefore, the resulting photonic biomaterials could be employed to construct nanoscale electronic devices applicable to future nanobiotechnology.

Received: November 2, 2010
Revised: March 30, 2011
Published online: May 20, 2011

Keywords: fibrous proteins · iron · photoelectric properties · phthalocyanines · self-assembly

[1] D. T. McQuade, A. H. Hegedus, T. M. Swager, *J. Am. Chem. Soc.* **2000**, *122*, 12389 – 12390.
[2] M. S. Choi, T. Yamazaki, I. Yamazaki, T. Aida, *Angew. Chem.* **2004**, *116*, 152 – 160; *Angew. Chem. Int. Ed.* **2004**, *43*, 150 – 158.
[3] C. X. Guo, H. B. Yang, Z. M. Sheng, Z. S. Lu, Q. L. Song, C. M. Li, *Angew. Chem.* **2010**, *122*, 3078 – 3081; *Angew. Chem. Int. Ed.* **2010**, *49*, 3014 – 3017.
[4] J. A. A. W. Elemans, R. van Hameren, R. J. M. Nolte, A. E. Rowan, *Adv. Mater.* **2006**, *18*, 1251 – 1266.
[5] C. M. Drain, A. Varotto, I. Radivojevic, *Chem. Rev.* **2009**, *109*, 1630 – 1658.
[6] Z. Wang, C. J. Medforth, J. A. Shelnutt, *J. Am. Chem. Soc.* **2004**, *126*, 16720 – 16721.
[7] P. J. Stang, B. Olenyuk, *Acc. Chem. Res.* **1997**, *30*, 502 – 518.
[8] C. F. van Nostrum, J. M. N. Roel, *Chem. Commun.* **1996**, 2385 – 2392.
[9] R. Takahashi, Y. Kobuke, *J. Am. Chem. Soc.* **2003**, *125*, 2372 – 2373.
[10] A. D. Baldwin, K. L. Kiick, *Biopolymers* **2010**, *94*, 128 – 140.
[11] C. A. Mirkin, R. L. Letsinger, R. C. Mucic, J. J. Storhoff, *Nature* **1996**, *382*, 607 – 609.
[12] E. Braun, Y. Eichen, U. Sivan, G. Ben-Yoseph, *Nature* **1998**, *391*, 775 – 778.
[13] H. Yan, S. H. Park, G. Finkelstein, J. H. Reif, T. H. LaBean, *Science* **2003**, *301*, 1882 – 1884.
[14] J. Richter, M. Mertig, W. Pompe, *Appl. Phys. Lett.* **2001**, *78*, 536 – 538.
[15] I. Cherny, E. Gazit, *Angew. Chem.* **2008**, *120*, 4128 – 4136; *Angew. Chem. Int. Ed.* **2008**, *47*, 4062 – 4069.
[16] T. Stromer, L. C. Serpell, *Microsc. Res. Tech.* **2005**, *67*, 210 – 217.
[17] S. Zhang, *Nat. Biotechnol.* **2003**, *21*, 1171 – 1178.
[18] M. Reches, E. Gazit, *Science* **2003**, *300*, 625 – 627.
[19] T. Scheibel, R. Parthasarathy, G. Sawicki, X.-M. Lin, H. Jaeger, S. L. Lindquist, *Proc. Natl. Acad. Sci. USA* **2003**, *100*, 4527 – 4532.
[20] M. Malisauskas, R. Meskys, L. A. Morozova-Roche, *Biotechnol. Prog.* **2008**, *24*, 1166 – 1170.
[21] M. Hamedi, A. Herland, R. H. Karlsson, O. Inganas, *Nano Lett.* **2008**, *8*, 1736 – 1740.
[22] E. N. Lee, H. J. Cho, C. H. Lee, D. Lee, K. C. Chung, S. R. Paik, *Biochemistry* **2004**, *43*, 3704 – 3715.
[23] M. Goedert, *Nat. Rev. Neurosci.* **2001**, *2*, 492 – 501.
[24] M. G. Spillantini, M. L. Schmidt, V. M.-Y. Lee, J. Q. Trojanowski, R. Jakes, M. Goedert, *Nature* **1997**, *388*, 839 – 840.
[25] G. Bhak, J.-H. Lee, J.-S. Hahn, S. R. Paik, *PLoS One* **2009**, *4*, e4177.
[26] J.-H. Lee, G. Bhak, S.-G. Lee, S. R. Paik, *Biophys. J.* **2008**, *95*, L16 – L18.
[27] J.-W. Park, J. S. Ahn, J.-H. Lee, G. Bhak, S. Jung, S. R. Paik, *ChemBioChem* **2008**, *9*, 2602 – 2605.
[28] M. Kasha , H. R. Rawls, M. A. El-Bayoumi, *Pure Appl. Chem.* **1965**, *11*, 371 – 392.
[29] G. Bhak, S. Lee, J. W. Park, S. Cho, S. R. Paik, *Biomaterials* **2010**, *31*, 5986 – 5995.